

Statistical Analysis of Clinical Phenotype and Patient Survival in Neurodevelopmental Disorder with Microcephaly, Arthrogryposis, and Structural Brain Anomalies

Dean Marchiori

A recently described, rare genetic condition known as Neurodevelopmental Disorder with Microcephaly, Arthrogryposis, and Structural Brain Anomalies (NEDMABA) has been identified in children with bi-allelic loss-of-function variants in *SMPD4*. The progression of this condition is not well understood with the limited case reports described so far exhibiting a severe and diverse clinical phenotype. A gap exists in the understanding the associations of the heterogenous features present in the clinical phenotype and the expected survival probabilities of affected individuals, driven in part to the paucity of analysis-ready data. This research aims to collate and standardise available case reports to analyse and identify meaningful clusters in the clinical phenotype, and to quantify the survival probability for children with NEDMABA. To overcome the challenge of sparse, multidimensional data on very few subjects, we employ Multiple Correspondence Analysis as a dimension reduction technique, which is then subject to hierarchical clustering and interpretation. To quantify more accurate survival probabilities, Kaplan-Meier estimation is formulated to account for censoring in the data. The analysis identified the classic phenotype for this condition, as well as two other distinct feature clusters. The first relates to findings of vocal cord paralysis and swallowing dysfunction, the other relates to more complex brain anomalies. Furthermore, the survival probability for those affected was found to decline sharply in early infancy, but exhibited a wide range of outcomes provisionally associated with variant type. However, interpretation of these results are guarded based on very low sample sizes. Ultra rare conditions present a challenge for clinicians and families, with often limited information and diverse possible outcomes. Despite challenges with sparse and inconsistent data, this analysis helps describe associations and trajectories of individuals with this condition and can provide clinicians and genetic counsellors with better information to aide in decision making and support for families.

Introduction

Neurodevelopment disorders are a diverse and heterogeneous group of conditions impacting the development of the nervous system, brain function, physical development, emotional development and learning ability. A recently identified condition known as Neurodevelopmental Disorder with Microcephaly, Arthrogryposis, and Structural Brain Anomalies (NEDMABA) (MIM:[618622](#)) has been described in children with bi-allelic loss-of-function variants in *SMPD4* (Magini et al. 2019). Sphingomyelinases such as *SMPD4* play an important cellular role by hydrolyzing sphingomyelin into ceramide and phosphorylcholine. *SMPD4* specifically encodes one of 4 neutral sphingomyelinases, nSMase3 (MIM: [610457](#)). So far, less than 50 cases of this rare disorder have been reported in the literature. Clinical phenotype data of these cases is largely heterogeneous with severe neurological complications and early demise a key feature. This makes the identification, diagnosis and ongoing management of cases a challenge for patients, their families and medical practitioners.

Ravenscroft et al. (2021) performed a study over 190 probands and identified a novel missense variation in *SMPD4* which at the time of whole exome sequencing was not well described in the literature. The impacted family from Melbourne exhibited features involving arthrogryposis multiplex congenita, complex brain malformations, small for gestation age and hypoplasia of the corpus callosum. In two of the three related cases were additional features of microcephaly, congenital encephalopathy, cerebellar malformation and hypoplasia and hypomyelination.

A detailed study by Magini et al. (2019) involved 12 unrelated families with 32 individuals (21 with detailed clinical information). Presentations were of microcephaly, simplified gyration, hypomyelination, thin corpus callosum, mild cerebellar hypoplasia, brainstem hypoplasia, congenital arthrogryposis, diabetes mellitus, heart disease, severe encephalopathy and respiratory problems often leading to early demise. Despite this being the largest cohort studied, the clinical features and survival times among participants varied greatly. Three missense changes were noted in the study with affected children in these families often showing a milder presentation suggestive of possible residual function. In these cases individuals were able to develop independent motor skills, have mild intellectual disability and arthrogryposis without evidence of simplified gyral patterns on brain MRI. Other patients with truncating variants are shown to have more severe presentations, while a range of additional significant clinical features were reported involving dysmorphic facial features, seizure, vocal cord paralysis and hearing impairment.

A case study from China is described in Ji et al. (2022) involving a girl presenting in infancy with intrauterine growth restriction, microcephaly, postnatal developmental delay, arthrogryposis, hypertonicity, seizure, and hypomyelination on brain magnetic resonance imaging. The authors report parallels with two cases showing the same homozygous null variant. An individual reported in Monies et al. (2019) presented with distinct symptoms of brain atrophy and skeletal dysplasia whereas the case in Magini et al. (2019) with the same variant exhibited more typical clinical features.

A recent study by Bijarnia-Mahay et al. (2022) presents the case of a 22-month old girl presenting with the typical phenotype of neurodevelopmental delay, prenatal onset growth failure, arthrogryposis, microcephaly and brain anomalies including severe hypomyelination, simplified gyral pattern and hypoplasia of corpus callosum and brainstem. Notably, there is also additional non-typical clinical findings of nystagmus and visual impairment secondary to macular dystrophy and retinal pigment epithelial stippling at posterior pole.

Further work to collate and analyse data relating to NEDMABA is challenging. While Magini et al. (2019) cataloged a detailed clinical phenotype data set as a supplementary data set to their study, these data are not suitable for statistical analysis as presented. Many of the clinical features are represented as free text descriptions and a variety of non-standard terminologies are applied between cases, making machine interpretation of the data difficult. Other studies (Ji et al. 2022; Bijarnia-Mahay et al. 2022) present only written case reports with some tabulated summaries. While larger studies (Ravenscroft et al. 2021; Monies et al. 2019) focus more on genetic data, with less detail included on the clinical presentation of individuals in the cohort.

To overcome these data challenges, Wickham (2014) proposes a data structure known as ‘tidy’ data which organises each observation in a row, with each feature as its own column and each value in just one cell. In this case detailed text-based data can be transformed to high dimensional binary indicators of key clinical features. This structure is conducive to effective statistical analysis and integrates deliberately with the *tidyverse* (Wickham et al. 2019) collection of packages for data analysis in R (R Core Team 2022).

Further analysis to better describe rare genetic conditions was explored in Díaz-Santiago et al. (2020) in the context of large scale genotype-phenotype analysis. The authors argue patients with rare disorders (often in small samples) often present with varied symptoms that do not match exactly with the described phenotype. When considering this situation of low sample size data with many features, methods in the field of multivariate statistical analysis are commonly deployed. Here the aim is to find substructure in the data, or a simple representation of the multi-dimensional space. Methods, such as Multiple Correspondence Analysis (Le Roux and Rouanet 2010) are appropriate for high dimensional data comprised of binary indicators. This technique is cited in many studies in the application of dimension reduction and clustering of comorbidities and phenotypes from disease (Han, Benseler, and Tyrrell 2018; Costa et al. 2013).

WIn terms of patient survival, methods in statistical survival analysis are well suited and commonly used in the field of genomics (Chen, Sun, and Hoshida 2014). These methods in particular provide a mechanism for dealing with right-censoring, a common feature of clinical studies where the clinical outcome of interest may not be known by the end of the study period. Within the context of examining a single condition, Crowe et al. (2020) investigated comorbidity phenotypes and mortality risk in ischaemic heart disease patients. Here latent class analysis was performed to identify a small number of clusters in the patients which could then be included in survival analysis techniques to better understand the comparative outcomes of patients of this condition.

An open research question exists around the clinical pathway and survival time of children exhibiting bi-allelic loss-of-function variants in SMPD4. With current research highlighting a diverse and heterogeneous phenotype, the relationship and correlations between these diverse features is not well understood. Furthermore, the survival time of affected children is not well understood despite early-demise featuring as a severe outcome. While a connection has been highlighted between some missense variants and a milder presentation with longer survival (Magini et al. 2019), this hypothesis has not been analysed further.

This research has three key aims. First, to collate and transform the variety of early case reports and studies on clinical phenotype data for this novel variant into an analysis-ready *tidy* data set. Secondly, to conduct analysis on the associations between commonly reported clinical features. Finally, to statistically quantify the expected survival time of children with NEDMABA based on the current case reports.

This will be the first in-depth analysis of early studies of this novel variant, which aims to produce statistical findings to better describe and understand this condition. This research will assist clinicians understand the typical and non-typical presentations of this challenging new condition. In addition, genetic counselling of families with affected children will benefit from enhanced analysis on outcomes of existing reported cases.

Methods

SMPD4 Data Package

The data contained in Magini et al. (2019) “Summary of SMPD4-Related Clinical Phenotype” is an excel spreadsheet tabulating each of the 21 individuals from the study with clinical details recorded. The file has 21 columns (one for each individual), and 64 rows (one for each phenotype or clinical remark).

The data were read into R (R Core Team 2022) without any changes, so as to preserve the reproducibility of the data transformation steps.

The data were transposed to ensure it could be presented as *tidy* formatted data (Wickham 2014). This requires:

1. Each variable (clinical phenotype) forms a column.
2. Each observation (individual) forms a row.
3. Each type of observational unit forms a table (every cell has just one item)

This resulted in a long-formatted data set of 21 rows (individuals) and 64 columns (clinical features).

In many cases, key clinical information was entered as free-text descriptions, which rendered any attempt of meaningful analysis impractical (Table 1). In these cases, the text was tokenised

by separating the list of clinical observations at each comma and forming a binary indicator column noting its presence ‘1’ or absence ‘0’ (Table 2).

Table 1: Example of non-tidy free-text descriptions of features

	Family 1- Individual 1	Family 1- Individual 4
Facial dysmorphisms	short palpebral fissures, large ears, simple helices, smooth philtrum, thin lips, bilateral simian creases	short palpebral fissures, receding forehead, thin upper lip

Table 2: Example of tidy formatted data where individuals are transposed into rows and text into binary indicators

id	short palpebral fissures	large ears	simple helices	receding fore- head	...
Family 1- Individual 1	1	1	0	...	
Family 1- Individual 4	1	0	0	1	...

In the case where two variables were formed from phenotypes that are considered to be synonymous, these were merged into one indicator column to prevent duplication e.g. {bilateral_cleft_lips, bilateral_cleft_lip, cleft_lip_b_l} -> {bilateral_cleft_lip}.

Some data type conversion and categorical level standardisation was performed to ensure the data were in consistent and appropriate data types. For example, ‘Gender’ was not consistently coded, and ‘Birth Weight’ was encoded as a text string rather than a more useful numeric format. (Table 3).

Table 3: Example of inconsistent coding or sub-optimal data types

Gender	Birth Weight
male	2175 grams (- 2.5 SD)
female	2045 g (-3 SD)
Female	2300 gram (-2 SD)
Female fetus	n.a.

Table 4: Example of consistent and appropriate coding or data types

Gender	Birth Weight (g)
male	2175
female	2045
female	2300
female	NA

This format was preserved and other case studies identified in the literature (Ravenscroft et al. 2021; Monies et al. 2019; Bijarnia-Mahay et al. 2022; Ji et al. 2022) were manually entered to conform to this template to allow the data to be combined for further analysis.

The final dataset consisted of 21 observations (one per individual) and 152 variables (one per clinical feature). In some cases, were obvious, these variables were left as qualitative character descriptions, in other cases as noted above, distinct lists of features were tranformed into binary indicators. Other fields include background information on the patient and various biomarkers. A full list of this data set is available in Table 8. These data sets were packaged into an R Package called SMPD4 (Marchiori 2022) in order to allow for reproducibility and sharing.

Multiple Correspondence Analysis

The data on subjects introduced above is subset to include only variables that can be transformed into binary indicator variables that represent the presence or absence of a given clinical feature column. Only those features that appeared in more than one case were included to minimise the influence of non-related features in this analysis.

Dimension reduction on this wide data set was performed using Multiple Correspondence Analysis (MCA) (Le Roux and Rouanet 2010) in order to arrive at a set of meaningfully small dimensions that account for most of the variation in the data. Multiple Correspondence Analysis (MCA) is an analogy to Principle Component Analysis (PCA) for categorical data.

We let these data be \mathbf{X} which is comprised of a set of individuals I and a set of features Q such that the q_{th} feature has K_q levels. The sum of all categories $K = \sum_{q=1}^Q K_q$ defines the dimensionality of \mathbf{X} as an $I \times K$ matrix. This resulted in a dataset $X_{28 \times 61}$ indicator matrix of 61 clinical features across 28 individuals. Taking $\delta_{ik} = 1$ if subject i has feature k and $\delta_{ik} = 0$ if the subject does not, we are left with the completely disjunctive table $\mathbf{X} = I \times K$ of $\{0, 1\}$. Letting the sum of all entries of \mathbf{X} be N , we have $\mathbf{Z} = N^{-1}\mathbf{X}$. We can introduce two diagonal matrices $\mathbf{D}_{\mathbf{r}} = \text{diag}(\mathbf{r})$ and $\mathbf{D}_{\mathbf{c}} = \text{diag}(\mathbf{c})$ where \mathbf{r} and \mathbf{c} are the vectors of row sums and column sums of \mathbf{Z} respectively.

Computing MCA involves taking the Singular Value Decomposition:

$$\mathbf{M} = \mathbf{D}_r^{-\frac{1}{2}}(\mathbf{Z} - \mathbf{r}\mathbf{c}^T)\mathbf{D}_c^{-\frac{1}{2}} = \mathbf{P}\Delta\mathbf{Q}^T$$

where Δ are the singular values and $\Lambda = \Delta^2$ is the matrix of eigenvalues.

This results in the row and column factor scores respectively as:

$$\begin{aligned}\mathbf{F} &= \mathbf{D}_r^{-\frac{1}{2}}\mathbf{P}\Delta \\ \mathbf{G} &= \mathbf{D}_c^{-\frac{1}{2}}\mathbf{Q}\Delta\end{aligned}$$

This computation of the Multiple Correspondence Analysis was computed using the *FactoMineR* R package (Lê, Josse, and Husson 2008).

The *contribution* of each category is computed for each of the principal axis per Le Roux and Rouanet (2010). This metric identifies the proportion of variance of that axis due to the point and is defined as:

$$Ctr_k = \frac{py_k^2}{\lambda}$$

Where p represents the point weighting, y is the coordinate relative to the principal axes of variance λ .

Cluster Analysis

The MCA coordinates for the first 4 principal dimensions were subject to clustering in order to find groups of features that were internally homogeneous and externally heterogeneous. This was computed in R using the *clValid* package (Brock et al. 2008).

A sensible range of clusters were trialed ranging from 2 to 7. Each of these settings were trialed across a range of clustering algorithms including AGNES hierarchical agglomerative (Kaufman and Rousseeuw 2009), Kmeans (Hartigan and Wong 1979) and self-organising maps (SOM) (Kohonen 2012).

The results for each method were evaluated using three internal cluster validation measures, Connectivity (Handl, Knowles, and Kell 2005), Silhouette width (Rousseeuw 1987) and Dunn Index (Dunn 1974).

The optimal method and cluster number was selected based on a trade off between the best performing method using the evaluation metrics and a sensible partitioning of the data for this analysis.

Survival Analysis

To model survival probability for all subjects in the combined data, the data are subsetted to include *survival_time* which is either the number of days the individual survived for, or the age in days at last follow up, and *deceased* a numeric indicator which is equal to 1 if the subject is deceased and 0 otherwise.

The Kaplan-Meier estimator (Kaplan and Meier 1958) is used to estimate the survival function of the data.

The estimator is calculated as:

$$\hat{S}(t) = \prod_{t_i \leq t} \frac{n_i - d_i}{n_i}$$

where t_i is some event time, d_i represents the number of events (here deceased subjects) and n_i indicating the individuals known to have survived up to t_i

The baseline estimator of all individuals was calculated using the *survival* package in R (Terry M. Therneau and Patricia M. Grambsch 2000).

Next the Kaplan-Meier estimator was calculated, [ON WHAT?] stratified by the reported type of Single nucleotide polymorphisms (SNP) reported in the literature. A test was performed to detect differences in the survival curves using methods from Harrington and Fleming (1982), again implemented in the *survival* package.

Finally, a Cox proportional hazards regression model (Andersen and Gill 1982) was fit on survival time with the variant type as the sole covariate. This was to detect and measure the Hazard ratio of variant type on the survival time in order to test the hypothesis that missense variant types exhibit significantly greater survival compared to other variant types.

Results

MCA

The initial results of the MCA were inspected with a bi-plot and identified two individuals (17, 18) from the data that were clear outliers and sat significantly beyond the 95% confidence ellipse. These individuals represented two twins from Magini et al. (2019) who were described with a much milder phenotype and were subject to a missense variation in SMPD4. Further analysis of this influence is conducted below. For now, these subjects were removed to allow for more meaningful analysis.

Repeating MCA for the remaining subjects shows the first dimension ($\lambda_1 = 0.18$) accounts for 17.88% of the variance in the data with the first 4 dimensions of the MCA analysis accounting for 54% of the variance (Table 5).

Table 5: Eigenvalues and percentage of variance explained by the MCA principal axes

MCA Eigenvalue Table			
Percentage variance explained by MCA for each dimension			
dimension	eigenvalue	percentage of variance	cumulative percentage of variance
dim 1	0.18	17.88%	17.88%
dim 2	0.14	13.81%	31.70%
dim 3	0.12	12.32%	44.01%
dim 4	0.10	9.66%	53.67%
dim 5	0.07	7.49%	61.16%
dim 6	0.06	5.97%	67.13%
dim 7	0.05	4.90%	72.03%
dim 8	0.04	4.20%	76.23%
dim 9	0.04	4.08%	80.31%
dim 10	0.03	3.47%	83.78%
dim 11	0.03	2.92%	86.70%
dim 12	0.02	2.49%	89.20%
dim 13	0.02	2.15%	91.34%
dim 14	0.02	1.82%	93.16%
dim 15	0.02	1.65%	94.81%
dim 16	0.01	1.12%	95.93%
dim 17	0.01	1.00%	96.93%
dim 18	0.01	0.93%	97.85%
dim 19	0.01	0.67%	98.53%
dim 20	0.01	0.63%	99.16%
dim 21	0.00	0.41%	99.57%
dim 22	0.00	0.31%	99.88%
dim 23	0.00	0.12%	100.00%
dim 24	0.00	0.00%	100.00%
dim 25	0.00	0.00%	100.00%

The *contribution* of the categories were ranked within each of the first four MCA dimensions See Figure 2.

The first dimension is dominated by highly specific facial dysmorphisms such as epicanthal folds, short philtrum and low anterior hairline. Also significant are seizure and developmental delay.

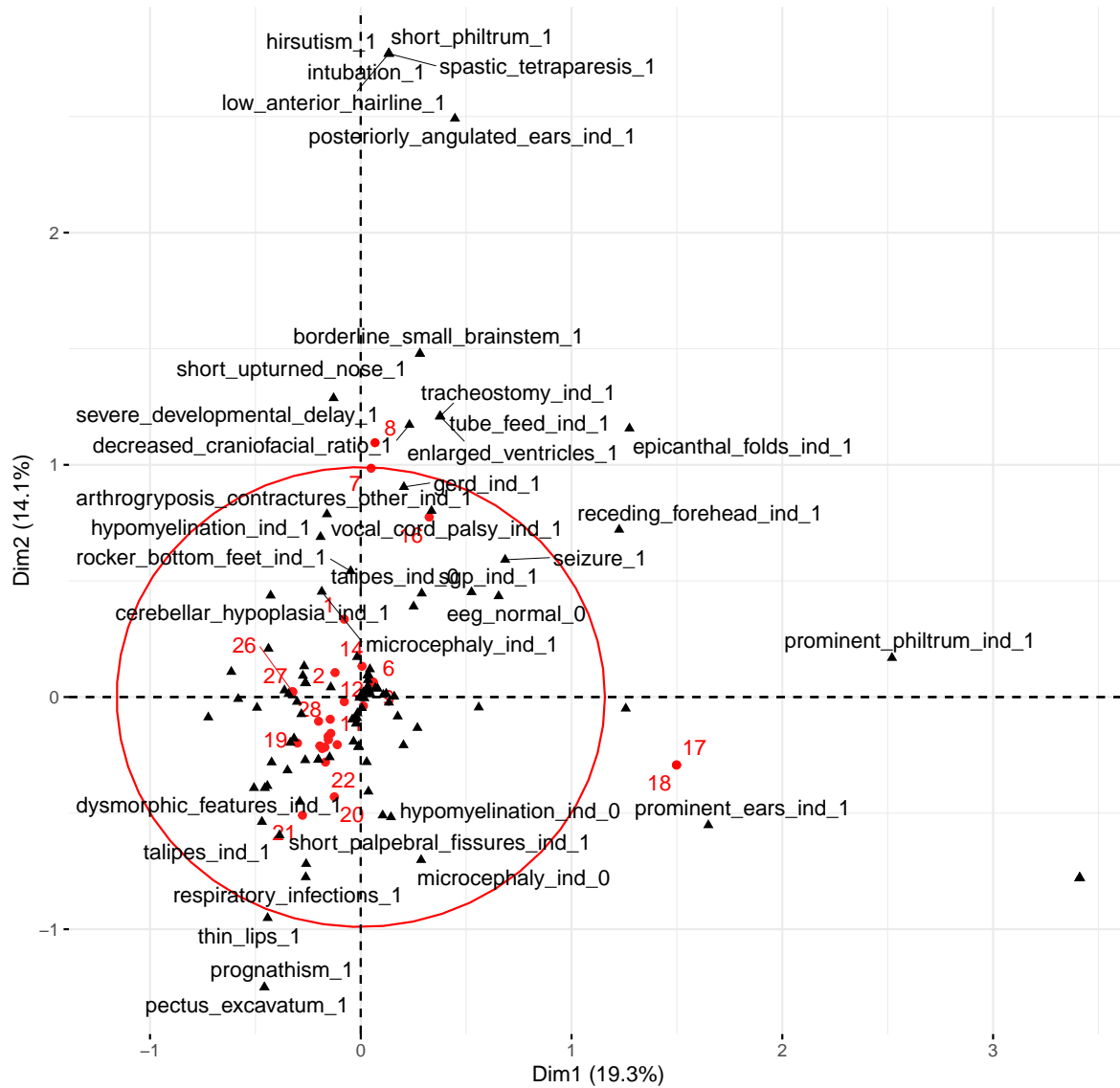


Figure 1: A bi-plot of the first two principal axes with grey circles indicating the individual's projected position and black triangles indicating the variables

The second MCA dimension is categorised by feeding and respiratory dysfunction with vocal cord palsy, tracheostomy, tube feeding and GERD.

Examining the bi-plot of the first two principal axes Figure 3 shows contrasting sources of variation between conditions relating to airway and swallowing function and predominantly structural brain anomalies such as cerebellar hypoplasia, agenesis of corpus collosum and development delay.

The third dimension is characterised by complex non-typical features such as patent ductus arteriosus, respiratory infections, small for gestational age and further facial features. These are contrasted by the fourth principal dimension which is typical for respiratory distress including stridor and hypercapnia.

Cluster Analysis

Internal cluster validation measures resulted in between 2 and 6 clusters as the optimal choice.

Proceeding with the optimal cluster selection, per the Silhouette coefficient of 6 clusters.

A scatterplot of the cluster results Figure 6 projected on just the first two dimensions highlights a core cluster of classic features of NEDMABA. A separate cluster is formed of airway and feeding related conditions involving vocal cord paralysis, tracheostomy, tube feeding and enlarged ventricles.

A cluster relating to structural brain anomalies is articulated with conditions such as cerebellar hypoplasia and agenesis of corpus collosum, along with small for gestational age.

Some smaller satellite clusters exist where highly distinctive features were associated with an individual or family. Also a singleton clusters exist for features that are distinct or unusual such as posteriorly angulated ears.

Table 6: Optimal clusters

Metric	Score	Method	Clusters
APN	0.07	agnes	2
AD	1.38	kmeans	5
ADM	0.33	kmeans	2
FOM	0.65	kmeans	5

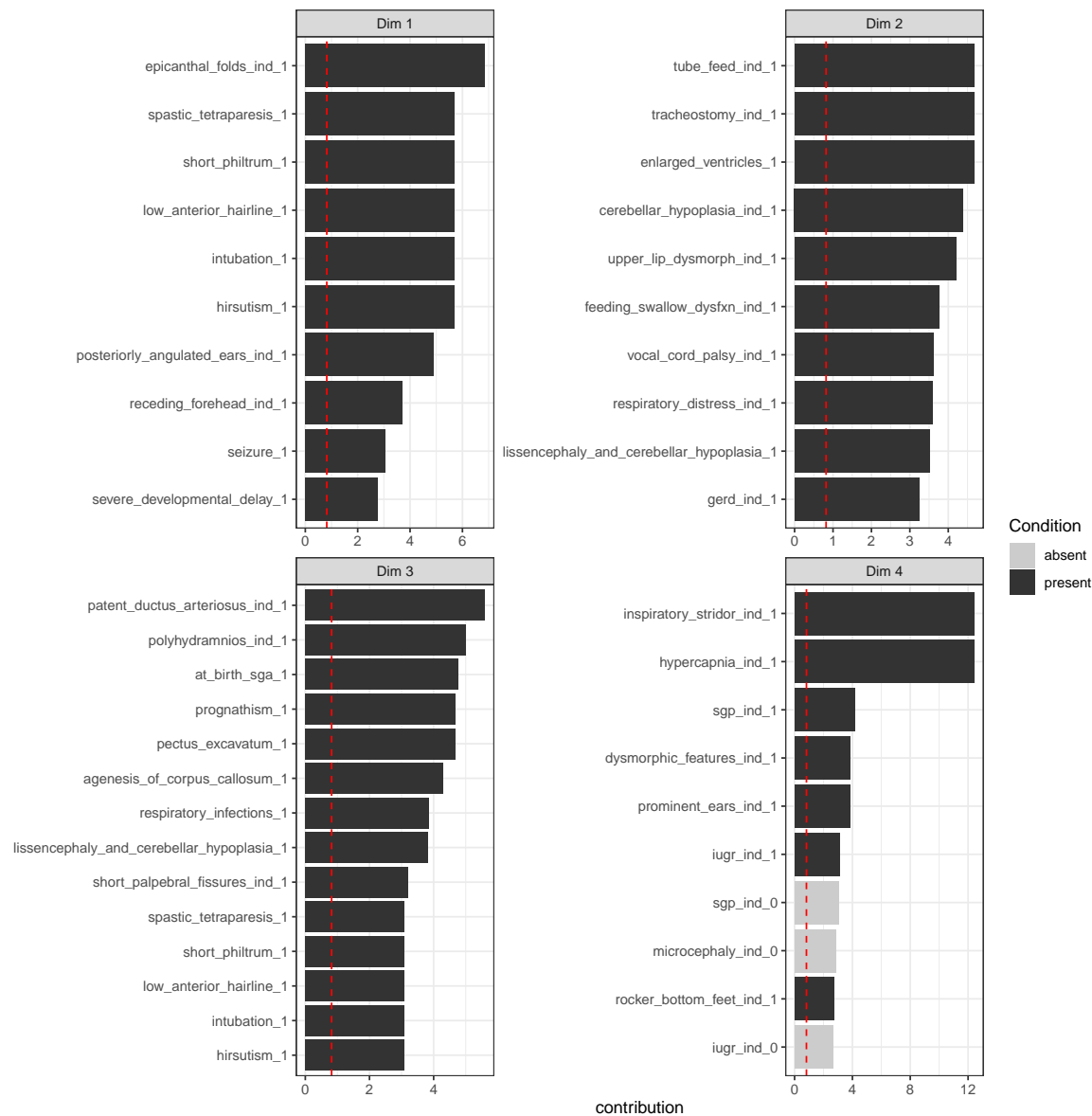


Figure 2: Top 20 feature categories from MCA analysis for the first four MCA dimensions. The red dashed line indicates the mean contribution value. Each feature may be present or absent as indicated by 1 or 0 respectively

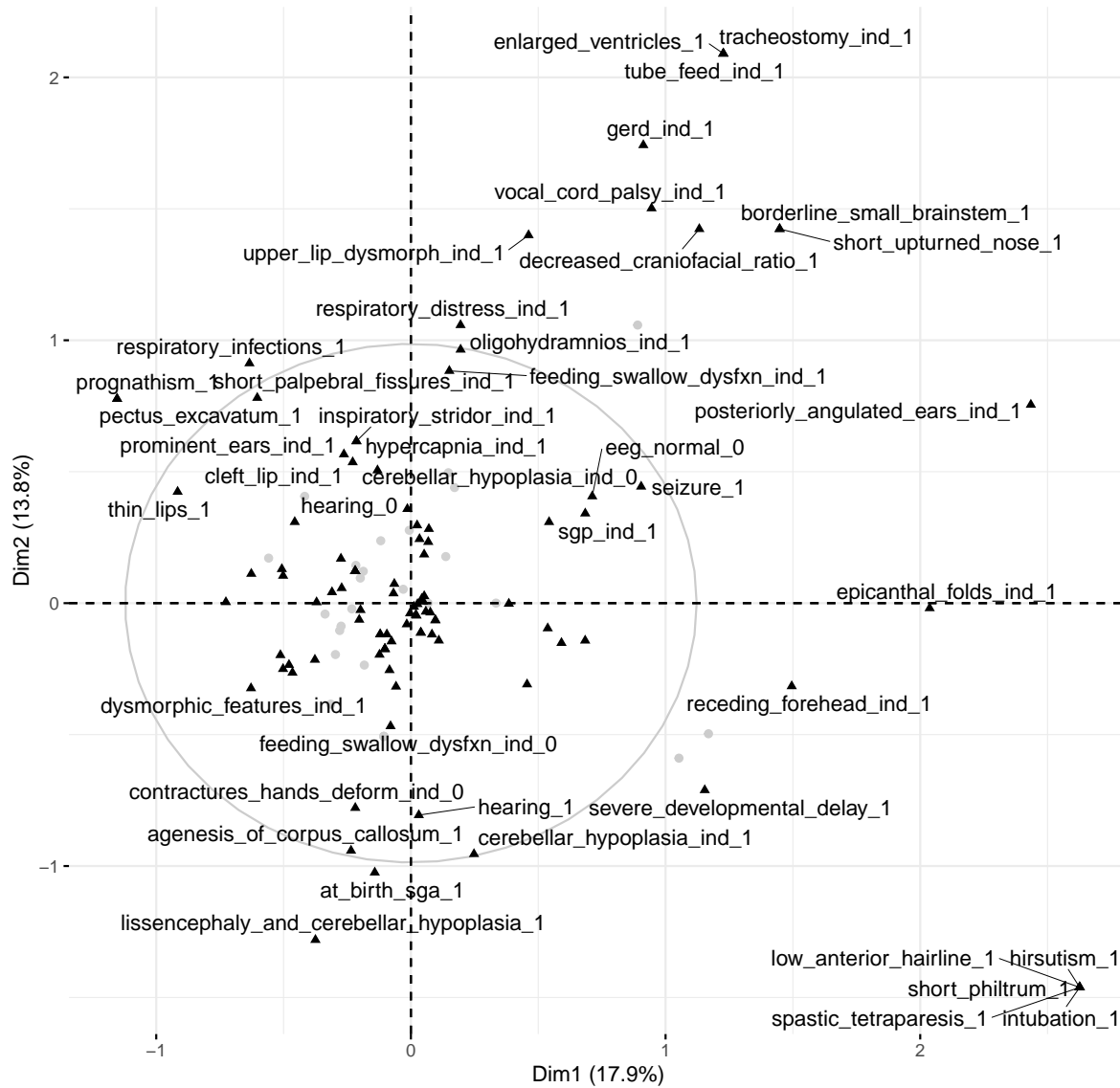


Figure 3: A bi-plot of the first two principal axes with grey circles indicating the individual's projected position and black triangles indicating the variables

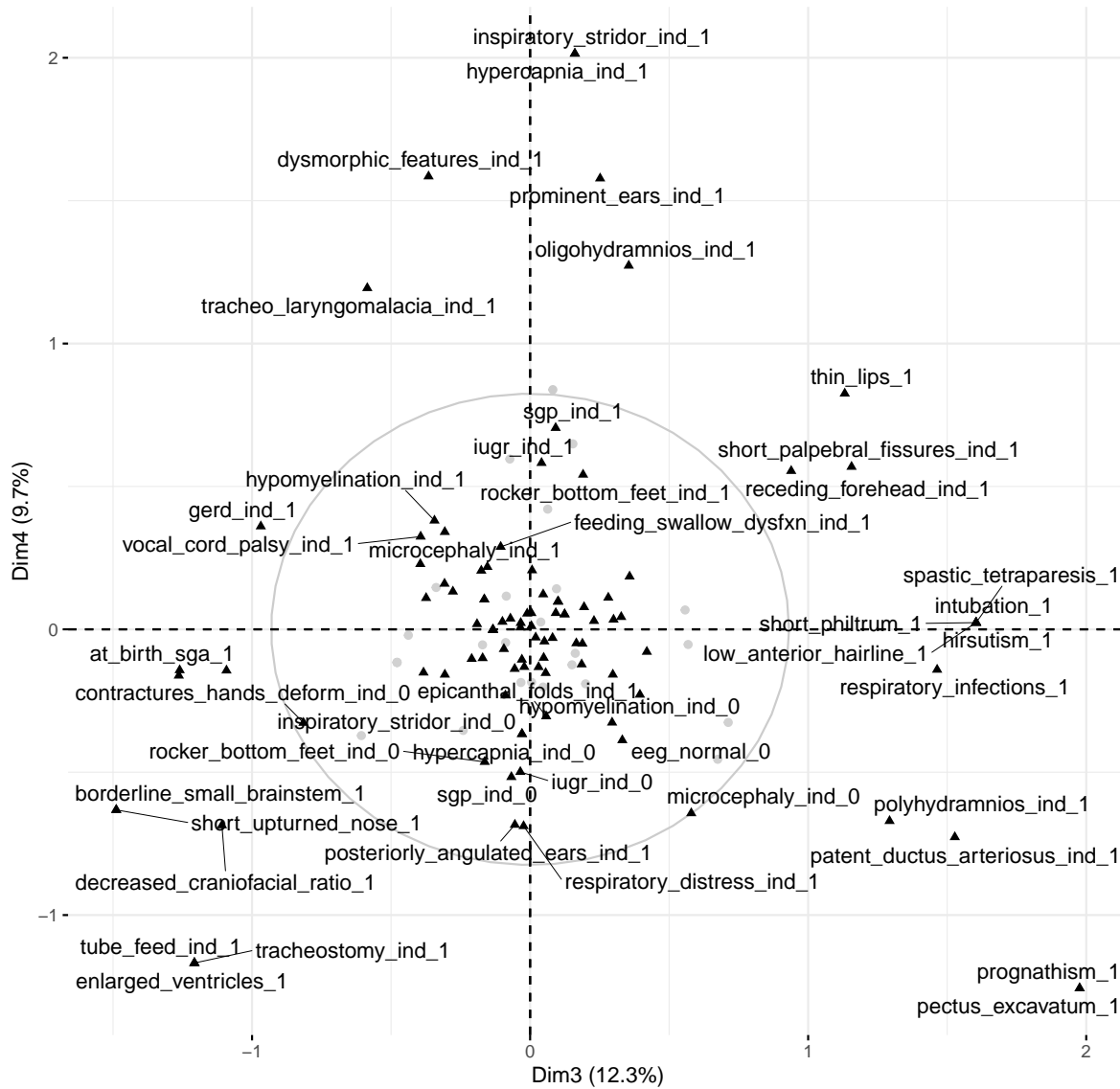


Figure 4: A bi-plot of principal axes 3 and 4, with grey circles indicating the individual's projected position and black triangles indicating the variables

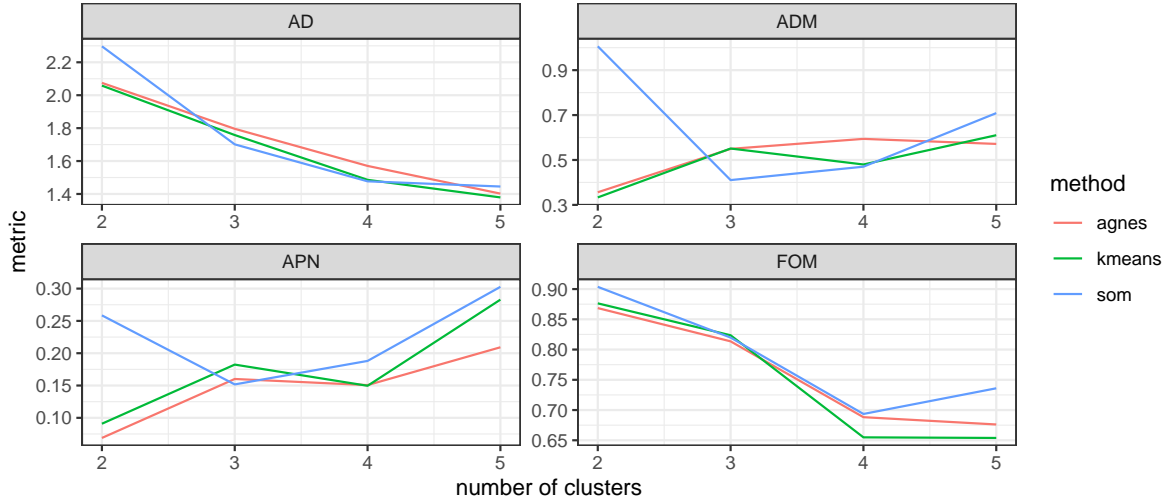


Figure 5: cluster validation analysis showing various metrics for cluster evaluation from 2 to 10 clusters. The most optimal number of clusters are selected by picking the lowest value from one or many of these comparable metrics.

Survival Analysis

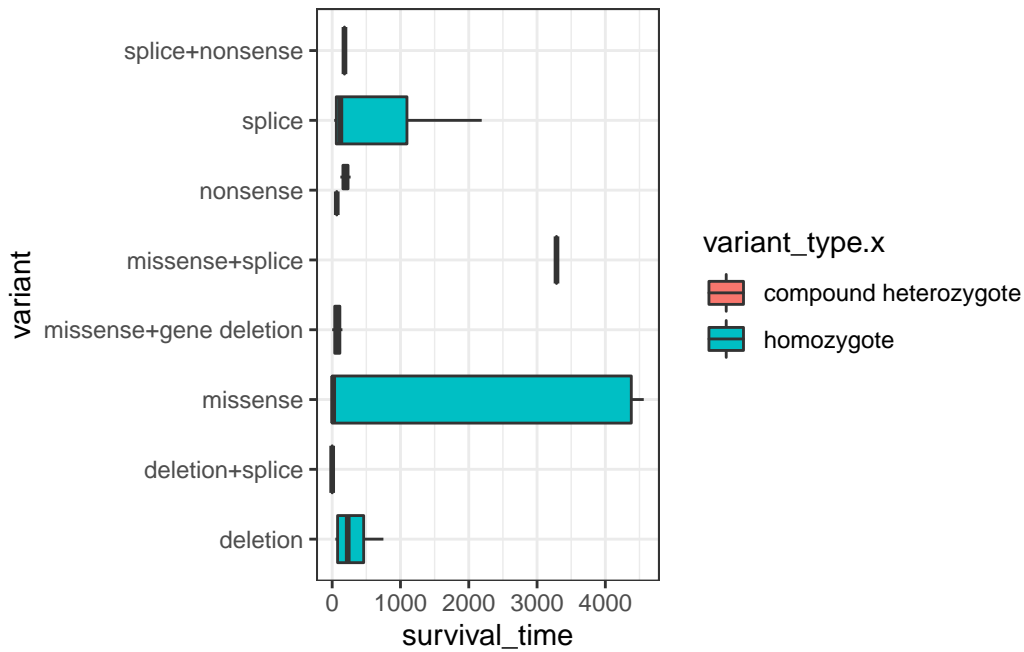
The Kaplan-Meier estimator shows a range of survival times (0, 4562 days) with survival probability at time 0 of 0.82 (0.69, 0.98). Survival probability after one year at 0.403 (0.252, 0.644) with median survival of 150 days and survival probability at close to ten years of 0.24 (0.11, 0.52).

Table 7: Survival probabilities derived from Kaplan-Meier estimation.

time	n.risk	n.event	n.censor	surv	std.err	upper	lower
0.0	28	5	0	0.82	0.09	0.98	0.69
15.0	23	1	0	0.79	0.10	0.95	0.65
30.0	22	2	0	0.71	0.12	0.90	0.57
47.0	20	1	0	0.68	0.13	0.88	0.53
60.0	19	1	1	0.64	0.14	0.85	0.49
67.0	17	1	0	0.61	0.15	0.82	0.45
90.0	16	0	1	0.61	0.15	0.82	0.45
120.0	15	2	0	0.52	0.18	0.75	0.37
150.0	13	1	0	0.48	0.20	0.72	0.33
180.0	12	1	0	0.44	0.22	0.68	0.29
240.0	11	1	0	0.40	0.24	0.64	0.25
270.0	10	0	1	0.40	0.24	0.64	0.25
365.0	9	0	1	0.40	0.24	0.64	0.25

time	n.risk	n.event	n.censor	surv	std.err	upper	lower
750.0	8	1	0	0.35	0.27	0.60	0.21
1095.0	7	1	0	0.30	0.31	0.56	0.16
1825.0	6	0	1	0.30	0.31	0.56	0.16
2190.0	5	1	0	0.24	0.39	0.52	0.11
3285.0	4	0	2	0.24	0.39	0.52	0.11
4380.0	2	1	0	0.12	0.81	0.59	0.02
4562.5	1	1	0	0.00	Inf	NA	NA

A comparative boxplot of survival times by variant type shows significant outliers for missense+splice and missense variations. However, even within missense homozygous variants the survival time varies greatly. Other missense variants, such as heterozygous missense with gene deletion do not show the same increased survival time as indeed noted by Magini et al. (2019).



The log rank test was carried out to compare the survival curves of the various gene variants $\chi^2 = 14.8$ ($p = 0.04$) however due to the small sample size, several variants had expected counts less than 5 which would create a violation in assumptions for the test.

Call:

```
survdif(formula = Surv(survival_time, deceased) ~ variant, data = survival_data)
```

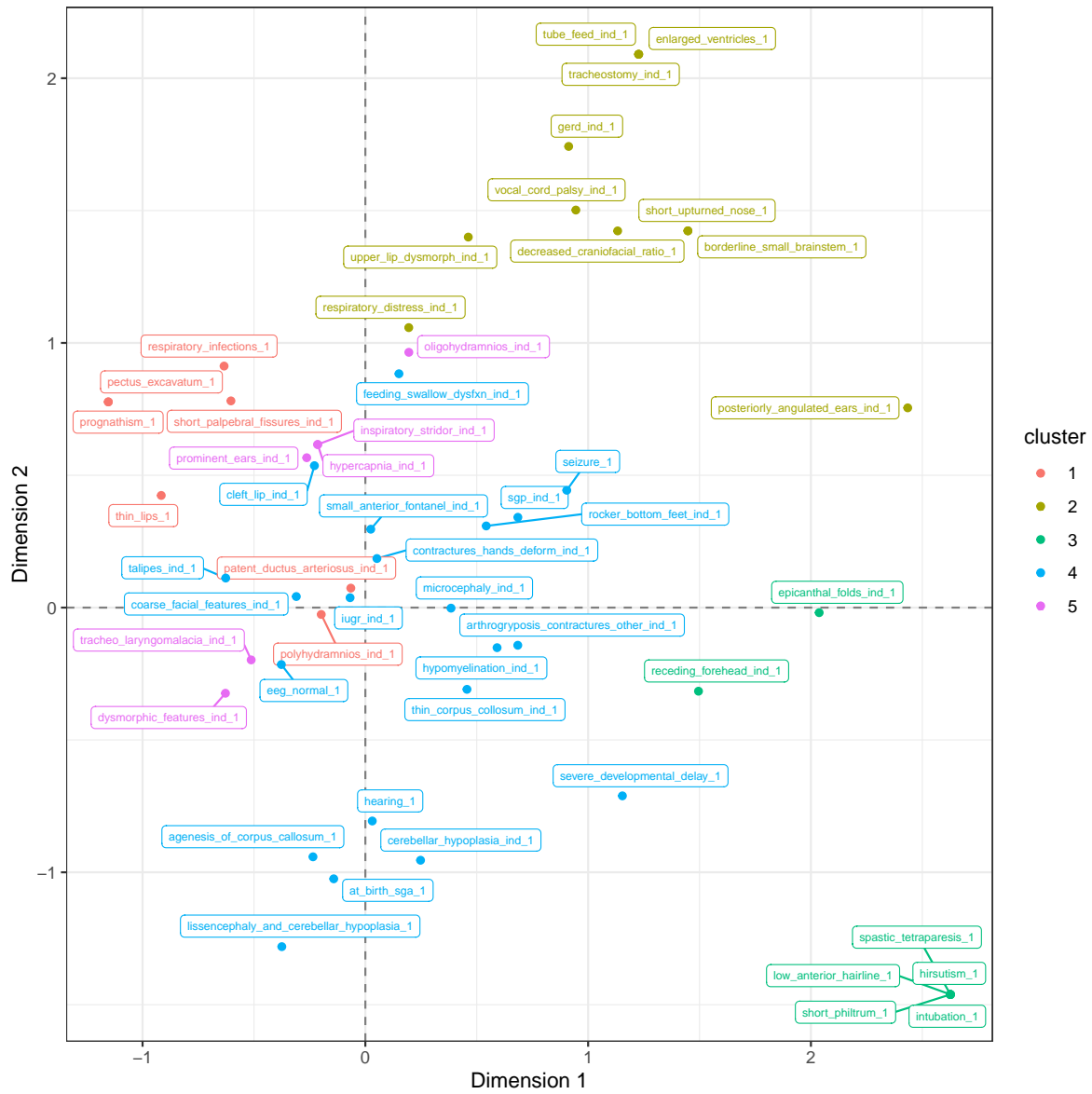



Figure 6: A projection of features on the first two principal components with cluster assignment indicated by colour.

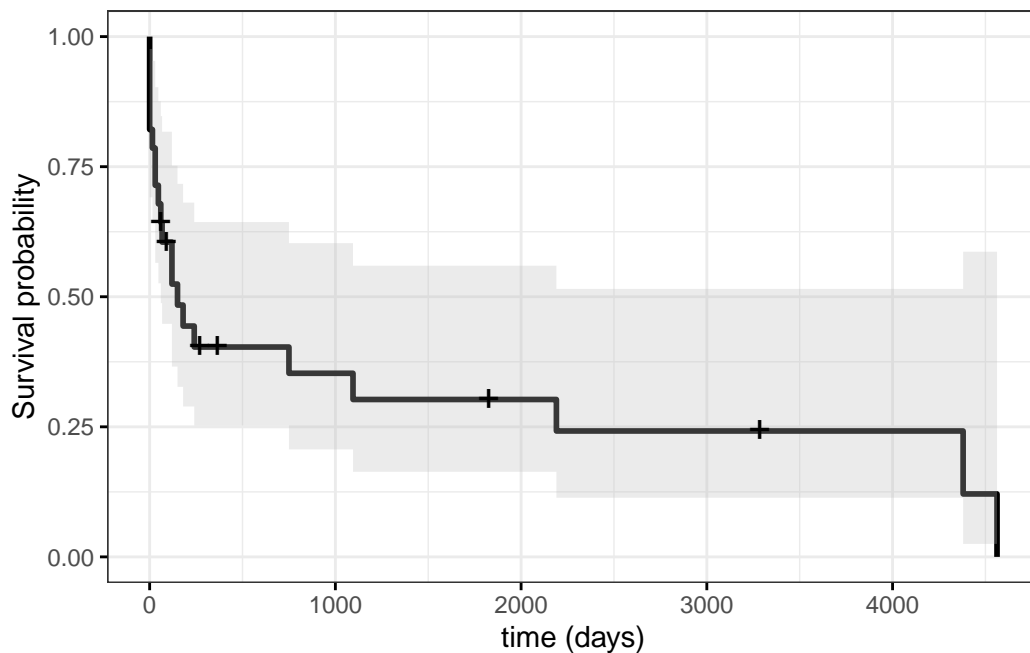


Figure 7: Kaplan Meier survival curve

	N	Observed	Expected	$(O-E)^2/E$	$(O-E)^2/V$
variant=deletion	4	2	2.680	0.17263	0.21735
variant=deletion+splice	2	2	0.357	7.55714	9.55385
variant=missense	5	5	5.233	0.01035	0.02213
variant=missense+gene deletion	2	2	0.863	1.49694	1.73215
variant=missense+splice	2	0	2.654	2.65354	3.39942
variant=nonsense	3	2	1.941	0.00179	0.00218
variant=splice	9	7	6.504	0.03781	0.06127
variant=splice+nonsense	1	1	0.768	0.07008	0.07839

Chisq= 14.8 on 7 degrees of freedom, p= 0.04

Discussion

The Multiple Correspondence Analysis confirmed the heterogeneous variation in the data with the first four principle components being required to explain more than 50% of the variation in the dataset.

The examination of key contributing factors, as well as a visual inspection of the dat projected into this lower dimensional space, indicate the primary sources of variation in the clinical

phenotype can be explained by few individuals with very different clinical features. This has confounded the typical or classical presentation.

Beyond these outliers, an interesting distinction is made between the hallmark features of microcephaly, hypomyelination, arthrogryposis, simplified gyral pattern and developmental delay with specific airway and swallowing features such as vocal cord paralysis, tracheostomy, GERD and tube feeding.

Further distinctions are possible with more specific structural brain anomalies exhibiting as distinct sources of variation in the clinical phenotype.

Many of the outlying features identified are specific facial or anatomical dysmorphisms. While a noted and core feature is around coarse facial features, those with a milder course had clinical reports in the available data that articulated these dysmorphisms in much more detail.

On a similar note, the reporting of ‘talipes’ as a condition seems distinct as a source of variation when appearing as an isolated feature without the typical microcephaly and hypomyelination. However, there was significant heterogeneity in how feet contractures were reported in clinical case reports. A distinction was made between reported cases with rocker bottom feet or congenital vertical talus and those with clubfeet/talipes. In practice it is not clear how these diagnoses were arrived at, and given the non-specific nature of this feature, care needs to be taken in distinguishing between similar manifesting features in the literature where possible.

The cluster analysis does not aim to group individuals that are alike, but rather the clinical features themselves. This highlights common sources of variation on the clinical phenotype of the condition itself, rather than typical coincident features of any one child. While the number of clusters chosen all represent valid partitions of the data, a larger number was selected to align the goals of the analysis which was to uncover distinct groups. A smaller number would have likely yielded isolated outliers from the main body of the features. This still occurs, however more substructure is detected with the higher cluster number.

In terms of patient survival, the first few months show a sharp decline in survival probability confirming early demise in the infant period as a key factor. A small number of cases show much longer survival into the childhood and in some cases into the second decade of life. The current literature suggests the type of gene variant has an impact on survival time, which seems to be supported in this work, however the limited sample size here prevents other meaningful analysis such as logrank tests or cox proportional hazard modelling which are likely underpowered when comparing multiple groups.

Despite NEDMABA exhibiting a diverse and heterogeneous clinical phenotype, it is possible to identify meaningful substructures in this data through the use of dimension reduction techniques (MCA) and cluster analysis. This has isolated the classic NEDMABA phenotype of microcephaly, hypomyelination, arthrogryposis, simplified gyral pattern and developmental delay. Furthermore it has isolated additional distinct groupings of features that are exhibited in patients such as vocal cord paralysis with tracheostomy, swallowing dysfunction, tube feeding

and GERD. In addition to typical MRI findings of symplified gyral pattern and hypomyelination, there exists clusters of structural anomalies of the corpus callosum and cerebella hypoplasia.

The survival of individuals with this condition is critical given early demise in infancy and childhood is a noted feature. This work identifies the survival probabilities and shows a one year survival rate of 0.403 (0.252, 0.644). A naive estimate, using just those number of deceased patients as proportion of the study population is 0.57. This highlights the importance of applying a survival analysis technique that incorporates censoring so as not to overestimate the survival probability.

Appendix

Table 8: Data dictionary of the final dataset used for the analysis. This combines the case reports and supplied data for available and references studies. The data has been transformed into a tidy format with formatting applied.

variable	type	description
study	character	.
id	character	.
family	character	.
individual	factor	.
deceased	logical	.
survival_time	numeric	.
variant_type	factor	.
locus_1	numeric	.
locus_2	numeric	.
gender	factor	.
ethnicity	character	.
consanguineous	logical	.
termination	logical	.
birth_gestation	numeric	.
route_vaginal_vs_c_sect	factor	.
birth_weight	numeric	.
birth_ofc	numeric	.
birth_length	numeric	.
age_at_demise	numeric	.
age_at_last_follow_up	numeric	.
microcephaly_ind	factor	.
sgp_ind	factor	.
iugr_ind	factor	.
talipes_ind	factor	.
rocker_bottom_feet_ind	factor	.
contractures_hands_deform_ind	factor	.
vocal_cord_palsy_ind	factor	.
arthrogryposis_contractures_other_ind	factor	.
hypercapnia_ind	factor	.
cleft_lip_ind	factor	.
inspiratory_stridor_ind	factor	.
polyhydramnios_ind	factor	.
coarse_facial_features_ind	factor	.
oligohydramnios_ind	factor	.

respiratory_distress_ind	factor	.
tracheostomy_ind	factor	.
prominent_ears_ind	factor	.
posteriorly_angulated_ears_ind	factor	.
prominent_philtrum_ind	factor	.
upper_lip_dysmorph_ind	factor	.
hypomyelination_ind	factor	.
cerebellar_hypoplasia_ind	factor	.
short_palpebral_fissures_ind	factor	.
epicanthal_folds_ind	factor	.
tube_feed_ind	factor	.
dysmorphic_features_ind	factor	.
patent_ductus_arteriosus_ind	factor	.
small_anterior_fontanel_ind	factor	.
receding_forehead_ind	factor	.
tracheo_laryngomalacia_ind	factor	.
gerd_ind	factor	.
thin_corpus_collosum_ind	factor	.
feeding_swallow_dysfxn_ind	factor	.
seizures_age_started	character	.
seizure_type_s	character	.
eeg	character	.
sleeping_problem	character	.
behavioral_issues	character	.
skeletal_changes_scoliosis	numeric	.
hip_luxation	numeric	.
development_head_control	character	.
sitting_unsupported	character	.
crawling	character	.
walking	character	.
speech	character	.
iq_int_disability	character	.
cp	character	.
performance	character	.
neuro_exam_eye_mvts_nystagmus	character	.
strabismus	character	.
feeding_swallow_dysfxn	character	.
gag	character	.
tone	character	.
strength	character	.
sensory_deficits	character	.
abnormal_mvts	character	.
dtr	character	.

other_neuro_signs	character	.
sensory_vision	character	.
hearing	character	.
other_organs	character	.
endocrinology	character	.
functional_tests	character	.
metabolic_investigation	character	.
cardiology	character	.
seizure	numeric	.
agenesis_of_corpus_callosum	factor	.
abnormal_pattern_of_cerebral_sulci	factor	.
left_sided_gallbladder	factor	.
suspected_brain_stem_dysfunction	factor	.
spastic_tetraparesis	factor	.
severe_developmental_delay	factor	.
acidosis	factor	.
small_thorax	factor	.
cyanosis	factor	.
intubation	factor	.
apnea	factor	.
mr_is_reportedly_with_migrational_defect	factor	.
at_birth_sga	factor	.
epilepsy_and_apnea	factor	.
choanal_atresia_surgeries_for_transposition_of_the_great_arteries	factor	.
interventricular_and_interatrial_defects	factor	.
smooth_philtrum	factor	.
thin_lips	factor	.
bilateral_simian_creases	factor	.
low_anterior_hairline	factor	.
short_philtrum	factor	.
prominent_nose_bridge	factor	.
depressed_nasal_bridge	factor	.
prominent_suture_ridges	factor	.
hypotelorism	factor	.
hypertrichosis_of_lower_back	factor	.
decreased_craniofacial_ratio	factor	.
there_is_overlapping_of_the_sutures	factor	.
bitemporal_narrowing	factor	.
short_upturned_nose	factor	.
short_neck	factor	.
upward_sweep_of_hair	factor	.
arched_eye_brows	factor	.
bulbous_nose	factor	.

prominent_lower_lip	factor	.
broad_chin	factor	.
prognathism	factor	.
asd	factor	.
left_multicystic_dysplastic_kidney	factor	.
anteriorly_placed_anus	factor	.
dilated_cardiomyopathy	factor	.
cryptorchidism	factor	.
hirsutism	factor	.
intestinal_malrotation	factor	.
dysphagia	factor	.
intermittent_sinus_bradycardia	factor	.
bilateral_staphylomas	factor	.
lissencephaly	factor	.
echogenic_choroid_plexus_on_head_us	factor	.
head_us_mild_ventriculomegaly	factor	.
brain_parenchyma_appears_homogeneous_without_evidence_of_focal_lesion	factor	.
hypoplastic_cerebellum	factor	.
borderline_small_brainstem	factor	.
abnormal_cerebellar_folia	factor	.
mild_vermian_hypoplasia	factor	.
asymmetry_of_lateral_ventricles	factor	.
lissencephaly_and_cerebellar_hypoplasia	factor	.
signs_of_hypoxic_encephalopathy	factor	.
mild_dilation_of_virchow_robins_spaces	factor	.
pectus_excavatum	factor	.
widely_spaced_nipples	factor	.
respiratory_infections	factor	.
enlarged_ventricles	factor	.
eeg_normal	numeric	.
bifid_uvula	factor	.
under_developed_cerebellar_inferior_vermis	factor	.

clust	var
1	polyhydramnios_ind_1
1	short_palpebral_fissures_ind_1
1	patent_ductus_arteriosus_ind_1
1	thin_lips_1
1	prognathism_1
1	pectus_excavatum_1
1	respiratory_infections_1

clust	var
2	vocal_cord_palsy_ind_1
2	respiratory_distress_ind_1
2	tracheostomy_ind_1
2	posteriorly_angulated_ears_ind_1
2	upper_lip_dysmorph_ind_1
2	tube_feed_ind_1
2	gerd_ind_1
2	decreased_craniofacial_ratio_1
2	short_upturned_nose_1
2	borderline_small_brainstem_1
2	enlarged_ventricles_1
3	epicanthal_folds_ind_1
3	receding_forehead_ind_1
3	spastic_tetraparesis_1
3	intubation_1
3	low_anterior_hairline_1
3	short_philtrum_1
3	hirsutism_1
4	microcephaly_ind_1
4	sgp_ind_1
4	iugr_ind_1
4	talipes_ind_1
4	rocker_bottom_feet_ind_1
4	contractures_hands_deform_ind_1
4	arthrogryposis_contractures_other_ind_1
4	cleft_lip_ind_1
4	coarse_facial_features_ind_1
4	hypomyelination_ind_1
4	cerebellar_hypoplasia_ind_1
4	small_anterior_fontanel_ind_1
4	thin_corpus_callosum_ind_1
4	feeding_swallow_dysfxn_ind_1
4	hearing_1
4	seizure_1
4	agenesis_of_corpus_callosum_1
4	severe_developmental_delay_1
4	at_birth_sga_1
4	lissencephaly_and_cerebellar_hypoplasia_1
4	eeg_normal_1
5	hypercapnia_ind_1
5	inspiratory_stridor_ind_1

clust	var
5	oligohydramnios_ind_1
5	prominent_ears_ind_1
5	dysmorphic_features_ind_1
5	tracheo_laryngomalacia_ind_1

References

- Andersen, Per Kragh, and Richard D Gill. 1982. “Cox’s Regression Model for Counting Processes: A Large Sample Study.” *The Annals of Statistics*, 1100–1120.
- Bijarnia-Mahay, Sunita, Puneeth H Somashekar, Parneet Kaur, Samarth Kulshrestha, Vedam L Ramprasad, Sakthivel Murugan, Seema Sud, and Anju Shukla. 2022. “Growth and Neurodevelopmental Disorder with Arthrogryposis, Microcephaly and Structural Brain Anomalies Caused by Bi-Allelic Partial Deletion of Smpd4 Gene.” *Journal of Human Genetics* 67 (3): 133–36.
- Brock, Guy, Vasyl Pihur, Susmita Datta, and Somnath Datta. 2008. “clValid: An R Package for Cluster Validation.” *Journal of Statistical Software* 25 (4): 1–22. <https://www.jstatsoft.org/v25/i04/>.
- Chen, Xintong, Xiaochen Sun, and Yujin Hoshida. 2014. “Survival Analysis Tools in Genomics Research.” *Human Genomics* 8 (1): 1–5.
- Costa, Patrício Soares, Nadine Correia Santos, Pedro Cunha, Jorge Cotter, and Nuno Sousa. 2013. “The Use of Multiple Correspondence Analysis to Explore Associations Between Categories of Qualitative Variables in Healthy Ageing.” *Journal of Aging Research* 2013.
- Crowe, Francesca, Dawit T Zemedikun, Kelvin Okoth, Nicola Jaime Adderley, Gavin Rudge, Mark Sheldon, Krishnarajah Nirantharakumar, and Tom Marshall. 2020. “Comorbidity Phenotypes and Risk of Mortality in Patients with Ischaemic Heart Disease in the UK.” *Heart* 106 (11): 810–16. <https://doi.org/10.1136/heartjnl-2019-316091>.
- Díaz-Santiago, Elena, Fernando M Jabato, Elena Rojano, Pedro Seoane, Florencio Pazos, James R Perkins, and Juan AG Ranea. 2020. “Phenotype-Genotype Comorbidity Analysis of Patients with Rare Disorders Provides Insight into Their Pathological and Molecular Bases.” *PLoS Genetics* 16 (10): e1009054.
- Dunn, Joseph C. 1974. “Well-Separated Clusters and Optimal Fuzzy Partitions.” *Journal of Cybernetics* 4 (1): 95–104.
- Han, Lu, Susanne M Benseler, and Pascal N Tyrrell. 2018. “Cluster and Multiple Correspondence Analyses in Rheumatology: Paths to Uncovering Relationships in a Sea of Data.” *Rheumatic Disease Clinics* 44 (2): 349–60.
- Handl, Julia, Joshua Knowles, and Douglas B Kell. 2005. “Computational Cluster Validation in Post-Genomic Data Analysis.” *Bioinformatics* 21 (15): 3201–12.
- Harrington, David P, and Thomas R Fleming. 1982. “A Class of Rank Test Procedures for Censored Survival Data.” *Biometrika* 69 (3): 553–66.
- Hartigan, John A, and Manchek A Wong. 1979. “Algorithm AS 136: A k-Means Clustering Algorithm.” *Journal of the Royal Statistical Society. Series c (Applied Statistics)* 28 (1): 100–108.
- Ji, Weigang, Xiangtian Kong, Honggang Yin, Jian Xu, and Xueqian Wang. 2022. “Case Report: Novel Biallelic Null Variants of Smpd4 Confirm Its Involvement in Neurodevelopmental Disorder with Microcephaly, Arthrogryposis, and Structural Brain Anomalies.” *Frontiers in Genetics* 13.
- Kaplan, Edward L, and Paul Meier. 1958. “Nonparametric Estimation from Incomplete Observations.” *Journal of the American Statistical Association* 53 (282): 457–81.

- Kaufman, Leonard, and Peter J Rousseeuw. 2009. *Finding Groups in Data: An Introduction to Cluster Analysis*. John Wiley & Sons.
- Kohonen, Teuvo. 2012. *Self-Organizing Maps*. Vol. 30. Springer Science & Business Media.
- Le Roux, Brigitte, and Henry Rouanet. 2010. *Multiple Correspondence Analysis*. Vol. 163. Sage.
- Lê, Sébastien, Julie Josse, and François Husson. 2008. “FactoMineR: A Package for Multivariate Analysis.” *Journal of Statistical Software* 25 (1): 1–18. <https://doi.org/10.18637/jss.v025.i01>.
- Magini, Pamela, Daphne J Smits, Laura Vandervore, Rachel Schot, Marta Columbaro, Esme Kasteleijn, Mees van der Ent, et al. 2019. “Loss of Smpd4 Causes a Developmental Disorder Characterized by Microcephaly and Congenital Arthrogryposis.” *The American Journal of Human Genetics* 105 (4): 689–705.
- Marchiori, Dean. 2022. *Smpd4: Smpd4-Related Clinical Phenotype Data*. <https://deanmarchiori.github.io/SMPD4>.
- Monies, Dorota, Mohammed Abouelhoda, Mirna Assoum, Nabil Moghrabi, Rafiullah Rafiullah, Naif Almontashiri, Mohammed Alowain, et al. 2019. “Lessons Learned from Large-Scale, First-Tier Clinical Exome Sequencing in a Highly Consanguineous Population.” *The American Journal of Human Genetics* 104 (6): 1182–1201.
- R Core Team. 2022. *R: A Language and Environment for Statistical Computing*. Vienna, Austria: R Foundation for Statistical Computing. <https://www.R-project.org/>.
- Ravenscroft, Gina, Joshua S Clayton, Fathimath Faiz, Padma Sivadorai, Di Milnes, Rob Cincotta, Phillip Moon, et al. 2021. “Neurogenetic Fetal Akinesia and Arthrogryposis: Genetics, Expanding Genotype-Phenotypes and Functional Genomics.” *Journal of Medical Genetics* 58 (9): 609–18.
- Rousseeuw, Peter J. 1987. “Silhouettes: A Graphical Aid to the Interpretation and Validation of Cluster Analysis.” *Journal of Computational and Applied Mathematics* 20: 53–65.
- Terry M. Therneau, and Patricia M. Grambsch. 2000. *Modeling Survival Data: Extending the Cox Model*. New York: Springer.
- Wickham, Hadley. 2014. “Tidy Data.” *Journal of Statistical Software* 59 (10): 1–23. <https://doi.org/10.18637/jss.v059.i10>.
- Wickham, Hadley, Mara Averick, Jennifer Bryan, Winston Chang, Lucy D’Agostino McGowan, Romain François, Garrett Grolemond, et al. 2019. “Welcome to the tidyverse.” *Journal of Open Source Software* 4 (43): 1686. <https://doi.org/10.21105/joss.01686>.